A Hydrodynamics-based Approach for Predicting the Blast Damage Zone in Drifting as Demonstrated Using Concrete Block Data

D.R. TESARIK[1] & W.A. HUSTRULID[2]

ABSTRACT

Rock falls involving a relatively small amount of material are a leading cause of injuries in underground mines in the United States. A contributing factor is unwanted blast damage and over-break. A goal of the United States National Institute for Occupational Safety and Health is to reduce the number of ground fall-related accidents by improving drift driving practices through the introduction of perimeter control blast designs. This paper presents a blast design technique based on a hydrodynamic method. Using commonly available explosive and geometry data, the theoretical particle velocity is calculated as a function of distance away from a cylindrical charge. A calibration factor is introduced to account for actual conditions by comparing the predicted values to a set of field data. The calibrated curve can then be applied for design. The paper introduces modifications to account for different explosives from those used in a calibration test. The application of the approach is demonstrated with respect to a data set from a large-scale concrete block test.

1. INTRODUCTION

Rock falls are one of the main causes of injuries in U.S. underground mines (MSHA 2006). Although the number of such accidents has decreased since reaching a peak in 1989, it has remained relatively constant for the past five years. Nearly all of these injuries involve relatively small pieces of rock falling from a zone about a half-meter thick surrounding the excavation (Bauer & Donaldson 1992, Mark & Iannacchione 2001). The total weight of the rocks in the majority of injury-caused rock falls is less than 11 kg (MSHA 2006). The widespread introduction of perimeter control blasting techniques in drift driving can potentially significantly reduce the number of these injuries. For this to occur, practical drift blast round design procedures including perimeter control must be made available to industry in a form which can be easily applied.

Holmberg and Persson (1979) have presented a perimeter control design technique based on the peak particle velocity generated by the detonation of a charge. Using the relationship between peak particle velocity (PPV), linear charge concentration,

[1]Address correspondence to: D.R. Tesarik, NIOSH-Spokane Research Laboratory, 315 E. Montgomery Ave, Spokane, WA 99207, det4@cdc.gov
[2]W.A. Hustrulid, NIOSH-Spokane Research Laboratory, 315 E. Montgomery Ave, Spokane, WA 99207, bte1@cdc.gov

distance from the charge, and the observed extent of damage, one obtains a limiting PPV value. This value can then be applied to the design curves to select explosive-hole combinations which yield acceptable perimeter damage. This method, known as the Holmberg-Persson method, has found quite wide acceptance. Unfortunately, a mathematical error was made in the development of the Holmberg-Persson equations (Hustrulid and Lu 2002). Iverson et al. (2008) introduced a modification in the Holmberg-Persson calculation procedure as a way of at least partially mitigating the problem. Blair and Minchinton developed the Scaled Heelen model which is similar in form to the Holmberg-Persson model, but uses full waveform superposition to calculate particle velocity at a given point (Blair and Minchinton 2006).

Other approaches for predicting the extent of damage are based on the gas pressure generated in the blasthole due to the explosion rather than the shock wave. Drukovanyi et al. (1976), for example, used the effect of the quasi-static expansion of detonating gases on brittle rock to derive equations for the radii of crushed and cracked zones surrounding a cylindrical charge.

Hustrulid and Johnson (2008) have produced two semi-empirical damage radius estimators based on the explosive gas pressure and the explosive energy, respectively. The pressure-based estimator can be applied to both fully-coupled and de-coupled charges. The importance of the buffer row design is stressed. They contend that if the buffer row is properly designed, the detailed design of the perimeter row becomes less important to overall perimeter control performance.

Vlasov (1957), Vlasov and Smirnov (1962), Kuznetsov (1974, 1977), Ill'inskii and Yakimov (1980), Ill'inskii and Potashev (1982), Kransov (1981), Nieman (1976, 1979, 1984a, 1984b, 1986a, 1986b) and others have applied a hydrodynamics-based approach to calculate theoretical particle velocity components at a given distance from a charge and this is the approach described here. This paper begins with a brief presentation of the basic equations pertaining to a cylindrical charge as originally presented by Nieman. The paper then continues by indicating how the equations can be modified to take into account actual rock behavior, and various explosives. The paper concludes by demonstrating the practical application of the approach to field data collected during a large concrete block test.

2. THEORETICAL DEVELOPMENT

2.1 Basic Assumptions

In the development of the equations it is assumed that (Hustrulid 1999):

- The detonation of the charge takes place in a confined space.
- As a result of detonation, the explosive charge is instantaneously transformed into a volume of gaseous products of the same size and shape as the space.

- In dense, monolithic rocks of high specific gravity and high ultimate rupture strength, the gaseous products do not substantially modify the properties of the rock prior to the completion of the detonation process.
- After detonation, some average pressure characteristic of the explosive type is established in the borehole.
- The medium surrounding the charge is considered to be uniformly deformable (linearly elastic) and incompressible. No account is taken of rock microstructure, fracturability, strength, or other properties.
- The medium will be considered isotropic with respect to all properties. This hypothesis is correct if it is considered that the in-homogeneities present in real rocks can, practically speaking, be equalized by the enormous pressure arising in the vicinity of the charge.
- The effect of the shock wave will be neglected. The amount of energy carried away by the shock wave is small compared to the total energy of the explosive and the zone of its action is insignificant.

Using the principles from hydrodynamics and these assumptions, one can calculate the particle velocity as a function of distance away from the charge. In reality, there are departures from these assumptions. For example, normal rock masses contain joints and other discontinuities which affect the incompressibility assumption. These are taken into account through a calibration procedure which will be demonstrated later in the paper.

2.2 Equation Derivation

The coordinate system shown in Figure 1 is used in developing the general expressions for the particle velocity field resulting from detonating a cylindrical charge in an infinite medium. As can be seen, the charge is oriented along the z axis and extends from z_1 to z_2.

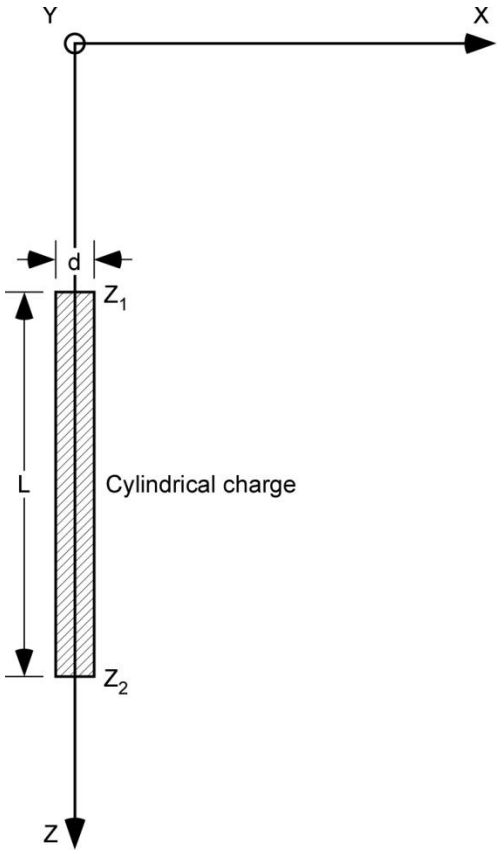

Fig. 1. Coordinate system for a cylindrical charge in an infinite medium.

The potential function developed by Nieman as presented in equation (1) will be used, which is

$$\phi = P \ln \frac{z_2 - z + \sqrt{x^2 + y^2 + (z_2 - z_1)^2}}{z_1 - z_2 + \sqrt{x^2 + y^2 + (z_1 - z)^2}}, \quad (1)$$

where

$$P = d \sqrt{\frac{\rho_e \, q_e}{8 \, \rho_m \, v_s}}, \quad (2)$$

d = diameter of the charge,
L = length of the charge,
ρ_e = density of the explosive,
q_e = energy/mass of the explosive,
ρ_m = density of the medium,

$$v_s = \ln \frac{\bar{L} + \sqrt{1 + \bar{L}^2}}{-\bar{L} + \sqrt{1 + \bar{L}^2}}, \text{ and} \quad (3)$$

. (4)

Taking derivatives of equation (1) with respect to x, y, and z, yields the velocity components u, v, and w, respectively:

$$u = P\,x\,(AB - CD) \tag{5}$$

$$v = P\,y\,(AB - CD), \text{ and} \tag{6}$$

$$w = P\,(C - A) \tag{7}$$

where

$$A = \frac{1}{\sqrt{x^2 + y^2 + (z_1 - z)^2}}, \tag{8}$$

$$B = \frac{1}{z_1 - z + \sqrt{x^2 + y^2 + (z_1 - z)^2}}, \tag{9}$$

$$C = \frac{1}{\sqrt{x^2 + y^2 + (z_2 - z)^2}}, \text{ and} \tag{10}$$

$$D = \frac{1}{z_2 - z + \sqrt{x^2 + y^2 + (z_2 - z)^2}}. \tag{11}$$

With the x-axis translated (re-positioned) to the mid-length position of the charge, the theoretical particle velocity u_t (oriented along the x axis) as a function of distance from the charge center can be expressed as

$$u_t = \sqrt{\frac{\rho_e\, q_e}{8\,\rho_m}}\;\frac{\bar{L}}{\sqrt{v_s}\;\bar{r}\sqrt{\bar{r}^2 + \frac{\bar{L}^2}{4}}}\;, \tag{12}$$

where

r = distance along the x axis from the center of the cylindrical charge and

$$\bar{r} = \frac{r}{d}. \tag{13}$$

Equation (12) can be written as

$$u_t = I\,\rho^{-1}, \tag{14}$$

where

$$I = \sqrt{\frac{\rho_e \, q_e}{8 \, \rho_m}} \text{ , and} \tag{15}$$

$$\rho = \frac{\sqrt{v_s} \, \bar{r} \sqrt{\bar{r}^2 + \frac{\bar{L}^2}{4}}}{\bar{L}} . \tag{16}$$

The geometric terms are all contained in the factor ρ while the rock and explosive parameters are contained in the multiplying constant I.

2.3 Required Modification for Actual Rock Masses

As indicated, in the derivation of the basic equations it has been assumed that the rock mass surrounding the charge is uniformly deformable (linearly elastic) and incompressible. No account is taken of rock microstructure, fracturability, strength, or other properties. However, rock masses, contain various types of structures on various scales and damage in the form of fracture development and extension develops during the blasting process. The associated deformations are not elastic except possibly in the far field. To obtain the required site specific design equations, a calibration blast is performed using an explosive charge of known geometry/properties in the given rock mass. The resulting PPV values are measured as a function of distance away from the charge. The field data would be expected to have the same form as Equation (14), but with a different coefficient (I_f) and exponent (α). One would write:

$$u_f = I_f \, \rho^{-\alpha}, \tag{17}$$

where

u_f = the field measured particle velocity perpendicular to and at mid-length to a single cylindrical charge.

The calibration factor K then becomes

$$K = \frac{u_f}{u_t} = \frac{I_f}{I} \frac{\rho^{-\alpha}}{\rho^{-1}} = \frac{I_f}{I} \rho^{1-\alpha} . \tag{18}$$

2.4 Modifications Based on Different Explosive Type

If an explosive is chosen for an application different than the one used in the calibration tests, one can easily produce a new predictor by modifying the ‘I’ factor.

Assume that 'I' applies for the original explosive and 'I'' for the new explosive. The theoretical particle velocity is then

$$u_t' = \frac{I'}{\rho}. \tag{19}$$

Solving for ρ in Equation (14) yields:

$$\rho = \frac{I}{u_t}. \tag{20}$$

By substituting this expression for ρ into Equation (19), one finds that the theoretical velocity resulting from the different explosive properties is

$$u_t' = \frac{I'}{I} u_t. \tag{21}$$

If it is assumed that field velocities are changed by the same ratio as theoretical velocities when the explosive term is changed, a first approximation for the equation for field velocity becomes

$$u_f' = \frac{I'}{I} I_f \rho^{-\alpha}. \tag{22}$$

3. DEMONSTRATION OF THE APPROACH

3.1 Introduction

As part of its overall program to advance cautious blasting principles, NIOSH has conducted a series of well-instrumented one-shot blasting tests in large monolithic concrete blocks (Iverson et al, 2009). This section illustrates the application of the hydrodynamic approach to the interpretation of the data and the development of a design curve.

3.2 Experiment Description

The concrete block experiment comprises a large concrete block measuring 2.4 m wide by 2.4 m long and 1.5 m high, a single blasthole, and an array of strain gage sensors placed at different distances away from the charge. The concrete block is intended to represent a homogeneous rock mass without structure. The concrete block is shown in Figure 2 prior to blasting.

Fig. 2. Photograph of block experiment prior to test showing placement of barrier blocks to restrain fly rock.

The physical properties are listed in Table 1.

Parameter	Value
Cohesion (MPa)	4.9
Internal friction angle (deg)	43
Uniaxial compressive strength (MPa)	21
Tensile strength, Brazilian (MPa)	1.75
Young's modulus, static (GPa)	13.1
Young's modulus, dynamic (GPa)	18.6
Poisson's ratio	0.25
Speed of sound, bar (m/sec)	2800
Speed of sound, block (m/sec)	3100
Density (kg/m3)	2000

Table I. Properties of the Concrete Block.

The blasthole (38 mm diameter) was percussion-drilled, nearly horizontal, and had a length of 1.8 m. It was collared at block mid-height with a burden of 0.45 m. The

blasthole was charged using Dyno® AP[1] (Dyno Nobel 2006). The explosive was tamped creating a fully coupled charge 1.2-m long measured from the hole-bottom. The charge extended to a distance of 0.6 m from the collar. Table 2 lists the properties for the explosive.

Parameter	Value	Units
Explosive density	1.15	g/cm^3
Detonation velocity	4300[a]	m/s
Diameter	31.75	mm
Tamped diameter	38.1	mm
Relative weight strength	0.88	
Relative bulk strength	1.00	
Energy	775	cal/g
	890	cal/cm^3
Tamped charge length	1.22	m
Total charge weight	1.60	kg

[a]Measured

Table II. Explosive properties.

The array of strain gages permitted measurement of strain attenuation with distance from the charge. Strain gage rosettes were embedded in the concrete at the same height as the blasthole. Because the block had been poured prior to deciding on the test design, instrument emplacement holes were diamond drilled at the appropriate locations. The strain gage rosettes were first bonded to the bottom ends of cured rectangular grout bars and the assembly was then grouted in the holes using the same grout. The grout had similar acoustic properties as the concrete to prevent wave reflection. The access holes were drilled at intervals of 23 cm away from the blasthole. A generalized plan view of the block experiment is shown in Figure 3. Although a rectangular grid of three strain gages was used at each location, only the results from the center, or radial strain gage were used. Each strain gage was connected to one arm of a Wheatstone bridge (quarter bridge configuration). The bridge output was connected to a Genesis data recorder manufactured by LDS Test and Measurement, Inc. Data were collected at the maximum rate of 1MHz.

[1] Mention of any company or product does not constitute endorsement by the National Institute for Occupational Safety and Health.

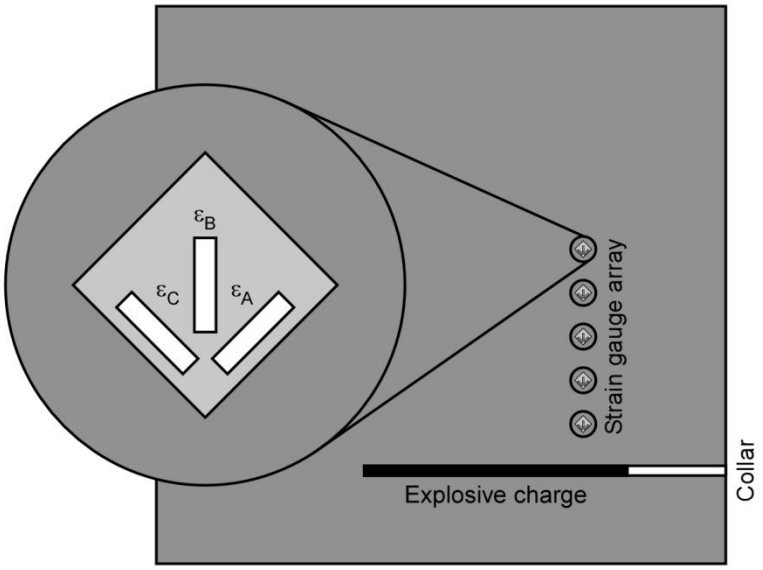

Fig. 3. Top view of block showing the locations of the strain gage array and the blasthole.

The measured peak radial strains as a function of distance are given in Table 3. The corresponding peak particle velocity (PPV) is calculated using the relationship

$$PPV = c\,\varepsilon_{peak}, \tag{23}$$

where

c = p-wave velocity (m/s) = 3100 m/s,
ε_{peak} = peak radial strain, and
PPV = peak particle velocity (m/s).

Distance (cm)	Peak strain	PPV (m/s)
22.9	.006475	20.1
45.7	.001592	4.9
68.6	.000691	2.1
91.4	.000332	1.0
114.3	.000288	0.9

Table III. Peak strain and PPV as a function of distance.

3.3 Data Analysis Using the Hydrodynamic Approach

The theoretical velocity equation developed by Nieman is

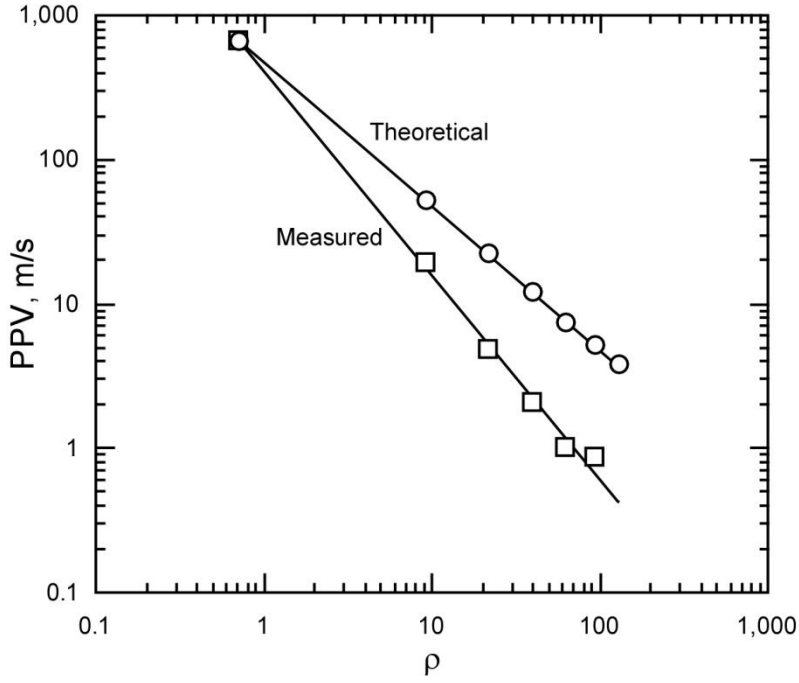

Fig. 4. Theoretical and measured velocity versus ρ for block test.

To plot the experimental results in the same fashion, one must determine the corresponding values of ρ for the measured particle velocities. This is done using equation (16).

$$\rho = \frac{\sqrt{v_s}\,\bar{r}\sqrt{\bar{r}^2 + \frac{\bar{L}^2}{4}}}{\bar{L}}$$

Since the length (L) and diameter (d) of the charge are, respectively

L = 1.2m, and
d = 0.038m,

one obtains,

$$\bar{L} = \frac{L}{d} = 31.58,$$

$$\bar{r} = \frac{r}{d} = \frac{r}{0.038},$$

$$v_s = \ln\frac{\bar{L} + \sqrt{1+\bar{L}^2}}{-\bar{L} + \sqrt{1+\bar{L}^2}} = \ln\left[\frac{31.58 + \sqrt{1+(31.58)^2}}{-31.58 + \sqrt{1+(31.58)^2}}\right] = 8.29\,,$$

and

$$\rho = \frac{\sqrt{v_s}\,\bar{r}\sqrt{\bar{r}^2 + \frac{\bar{L}^2}{4}}}{\bar{L}} = \frac{\frac{r}{0.038}\sqrt{8.29}\sqrt{\left(\frac{r}{0.038}\right)^2 + \frac{1}{4}(1.58)^2}}{31.58}$$

or

$$\rho = 2.399\, r\sqrt{\left(\frac{r}{0.038}\right)^2 + 249.32} \qquad (25)$$

At the wall of the hole, r = 0.019 m, the corresponding value of ρ is found using equation (25). For this case one obtains,

$$\rho = 0.72$$

The theoretical velocity at the wall of the hole is

$$u_{tw} = 483\,\rho^{-1} = 483(0.72)^{-1} = 670\ m/s\,. \qquad (26)$$

The calculated values of ρ for the measurement point locations and the associated PPV values are given in Table 4.

Distance (cm)	ρ	PPV (m/s)
22.9	9.29	20.1
45.7	21.90	4.9
68.6	39.48	2.1
91.4	63.10	1.0
114.3	93.18	0.9

Table IV. Calculated values of ρ for measurement point locations and associated PPV.

These experimental values are plotted in Figure 4. As can be seen, the points are well described by a straight line on log scales with the equation

$$u_f = 414\,\rho^{-1.416}\,. \qquad (27)$$

The calculated velocity of 659 m/s at the hole wall is very similar to the theoretical value (670 m/s).

A calibration factor (K) relating the theoretical and experimental velocity curves is obtained by dividing equation (14) by equation (27):

$$K = \frac{u_t}{u_f} = 1.16\,\rho^{0.416}\,. \qquad (28)$$

The expected velocities (u_e) for other charge diameters and lengths can then be obtained using

$$u_e = \frac{I\,\rho_e^{-1}}{K} = \frac{I\,\rho_e^{-1.416}}{1.16}, \tag{29}$$

where

$$\rho_e = \frac{\sqrt{v_{es}}\,\overline{r_e}\sqrt{\overline{r_e}^{\,2} + \frac{\overline{L_e}^{\,2}}{4}}}{\overline{L_e}}. \tag{30}$$

Since the explosive, the charging conditions and the rock mass remains the same, the value of I remains constant.

Design curves of the form PPV versus distance, r, are developed by using Equations 29 and 30. Figure 5 is a plot of PPV versus distance for the 1.2-m long fully-coupled cylindrical charge with diameter 38mm. Figure 6 shows the curves for fully-coupled charges 25mm, 38mm, 50mm, 64mm and 76mm in diameter. These data are plotted on normal scales in Figure 7.

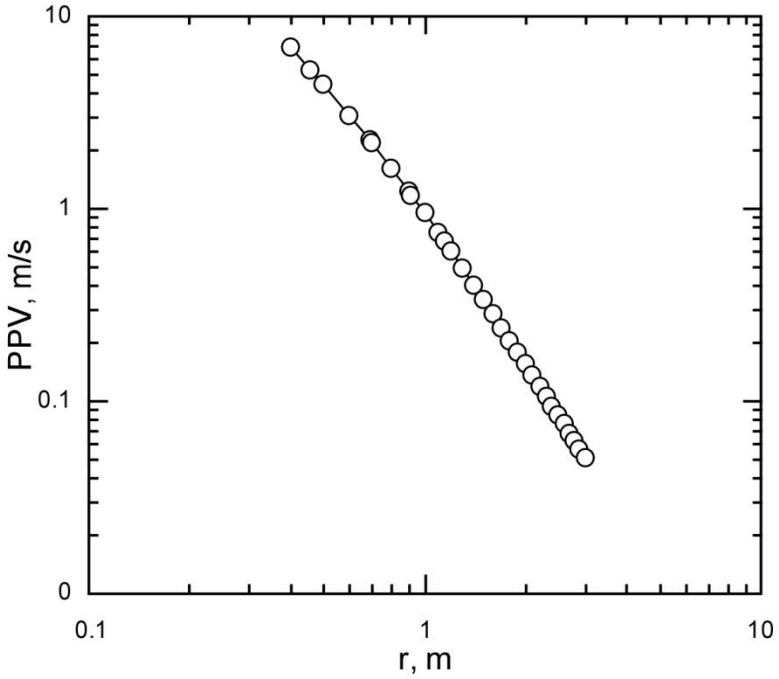

Fig. 5. Design curve for 1.2-m long fully-coupled cylindrical charge with diameter 38 mm.

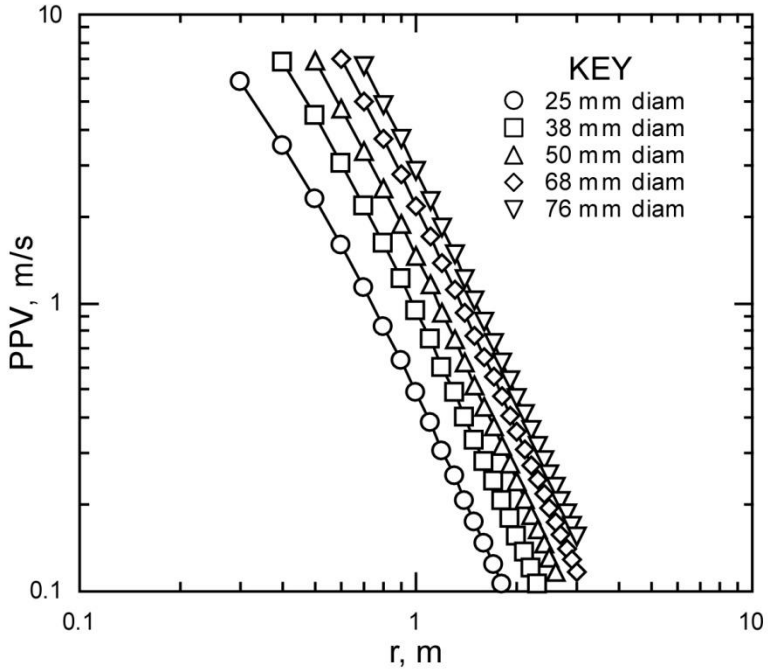

Fig. 6. Design curves for 1.2-m long fully-coupled cylindrical charges using log scales.

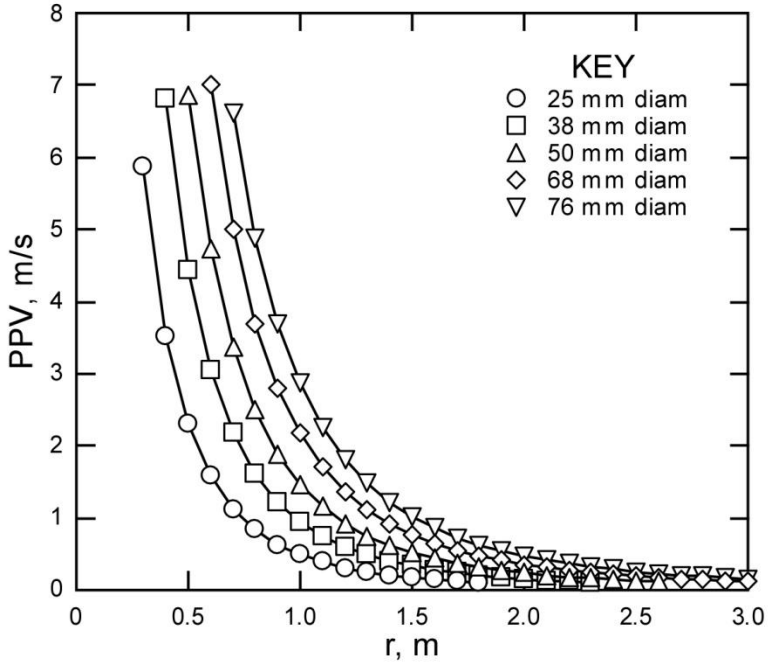

Fig. 7. Design curves for 1.2-m long fully-coupled cylindrical charges using normal scales.

3.4 Damage Assessment

Several different techniques were used to assess the extent of blast damage. An NX (78mm) diameter diamond drill hole was drilled specifically for this purpose. The change in s-wave velocity in the hole wall was observed as a function of distance away from the charge using a Micro-Velocity Probe (MVP). One set of results is shown in Figure 8. As can be seen, the apparent damage zone is of the order of 50 cm. This value is defined as the crushed zone for purposes of this paper. Cross core sonic (p-wave) and Brazilian tensile strength tests performed on the recovered core yielded similar damage zones.

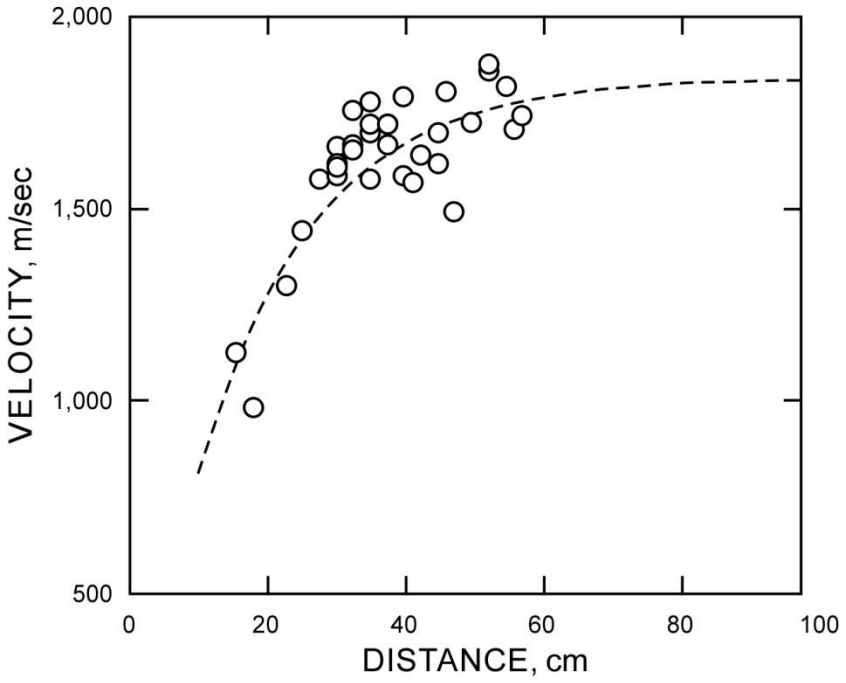

Fig. 8. Shear wave velocity as a function of distance from the hole.

After the blast, several wire-saw cuts oriented normal to the charge axis were made through the remaining block. The maximum crack limit was determined by visual inspection of the saw cut surfaces. Figure 9 presents the results from one of the cuts. As shown, the maximum crack length on this section is 176 cm. In summary, the measurements indicate a crush limit of the order of 50 cm measured radially from the center of the column charge and a crack limit extending to 176 cm. These damage limits are specific to the concrete material and the explosive tested.

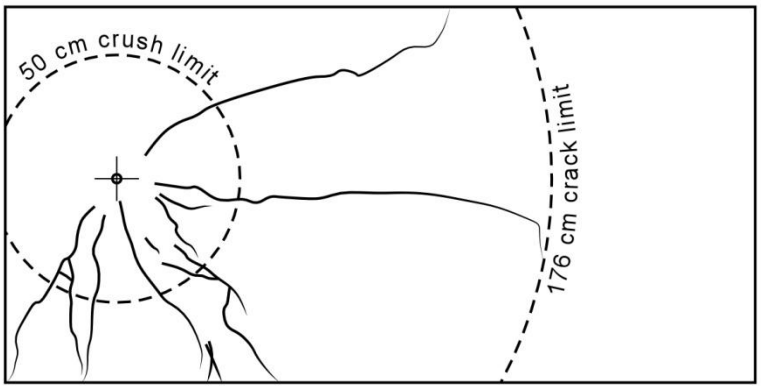

Fig. 9. Wire saw section showing the cracking.

Superimposing the observed damage limits on Figure 5, one finds that the approximate limiting PPV limits for crushing and cracking are 4.40 m/s and 0.22 m/s, respectively, as shown in Figure 10.

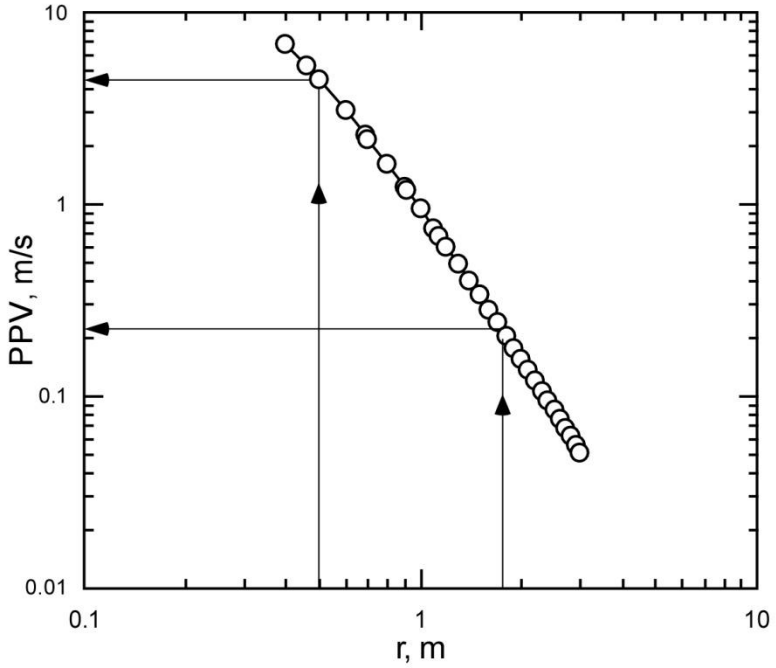

Fig. 10. PPV versus distance from charge for a 1.2-m long, 38 mm diameter charge with the damage limits determined.

These limits are now superimposed on the set of design curves in Figure 11. The crushing and cracking limits for the different charge diameters are given in Table 5.

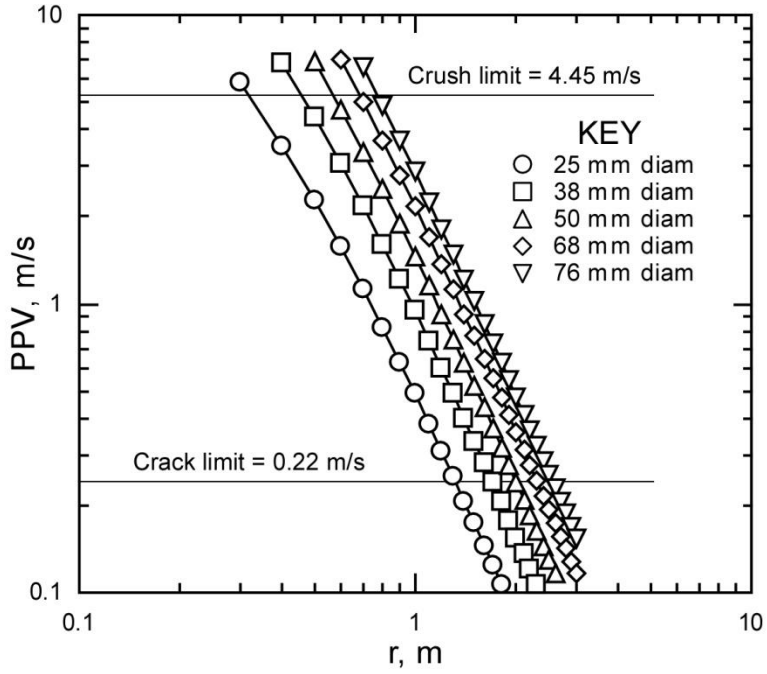

Fig. 11. Design curves with crushing and cracking limits.

Charge diameter (mm)	Crushing limit (m)	Cracking limit (m)
25	0.35	1.38
38	0.50	1.76
50	0.62	2.10
64	0.74	2.40
76	0.82	2.60

Table V. Crushing and Cracking limits.

4. Summary and Conclusions

The hydrodynamic approach for predicting the extent of blast damage caused by an explosive charge in an idealized rock mass as characterized by the peak particle velocity (PPV) has been described. A calibration factor is introduced to account for the actual behavior of the explosive in a particular rock mass. This factor is obtained by conducting a field test in which particle velocity measurements are made as a function of distance away from the charge. Once the calibration factor has been determined, PPV versus distance curves can be easily constructed for different explosive charge – hole combinations. By observing the extent of damage for a given rock – explosive combination and making use of the appropriate PPV versus distance curve, one can determine the limiting PPV for a particular damage type. By adding these limits to the calibrated PPV versus distance curves, one obtains a very simple approach for developing drift round blast designs with a certain maximum extent of perimeter damage. The

practical application of the approach has been demonstrated using data from a single hole blast in a large concrete block.

In summary, the approach appears to be fundamentally sound and quite easy to apply. Provided that the calibration test is conducted in a representative section of the rock mass, this method could be used to design perimeter charges and improve underground mine safety by reducing overbreak. Further calibration tests in rock masses containing various joint characteristics and other discontinuities are needed.

Acknowledgments

The authors wish to thank Jeff Johnson, Steve Iverson, Carl Sunderman, Ed McHugh, Ted Williams, Paul Pierce, Ron Jacksha, Mike Stepan, Rich Rains, and Brian Stapleton, NIOSH, SRL for conducting the concrete block and material property tests. Mark Johnson, Northwest Contractors, and Troy Knutti and James Zweirs, Dyno Nobel conducted the blast. Their work is greatly appreciated.

References

Bauer G. & D. Donaldson (1992) Perimeter control in development and breasting by use of a blasting program readily accepted by miners. In: Proceedings of the 18th Annual Conference on Explosives and Blasting Technique, International Society of Explosive Engineers, p. 133-140, Cleveland.

Blair, D.P. & A. Minchinton (2006) Near-field blast vibration models. In: Proceedings of the 8th International Symposia on Rock Fragmentation by Blasting, Asociación Chilena de Ingenieros Explosivistas de Chile A.G. (ASIEX), p. 152-159, Santiago.

Drukovanyi, M.F. (1976) Calculation of fracture zones created by exploding cylindrical charges in ledge rocks. Soviet Mining Science, 12(3): 292-295.

Dyno Nobel Inc. (2006) Explosive Engineer's Guide.

Holmberg R. & P.A. Persson (1979) Design of tunnel perimeter blasthole patterns to prevent rock damage. In: Proceedings Tunnel '79 (Ed.: Jones, M.J.), p. 280-283, IMM, London.

Hustrulid, W. (1999) Blasting Principles for Open Pit Mining Volume 2 - Theoretical foundations. Balkema, Rotterdam.

Hustrulid, W. & Lu, W. (2002) Some general design concepts regarding the control of blast-induced damage during rock slope excavation. In: Proceedings of the Seventh International Symposium on Rock Fragmentation by Blasting (Ed.: Wang, X.), Beijing Metallurgical Industry Press, Beijing. pp. 595 – 604.

Hustrulid W. & J. Johnson (2008) A gas pressure-based drift round blast design methodology. In: Proceedings of the 5th International Conference on Mass Mining (Eds.: Achunnesson H, & E. Nordlund), p. 657-669, University of Technology Luleå, Luleå.

Ill'inskii, N.B. & N.D. Yakimov (1980) Interaction between two buried fuse charges during ejection blasting. Soviet Mining Science. 16(2): 107-113.

Ill'inskii, N.B. & A.V. Potashev (1982) Mathematical modeling of the energy characteristics of a charge in pulsed-hydrodynamic models of a throwout explosion. Soviet Mining Science. 18(1): 36-44.

Iverson, S. et al. (2008) Application of the NIOSH-Modified Holmberg-Persson Approach to Perimeter Blast Design. In: Proceedings of the 34th Annual Conference on Explosives and Blasting Technique, 33 pp., International Society of Explosive Engineers, Cleveland.

Iverson, S.R. et al. (2009) Experimental determination of the extent of blast damage from a fully coupled explosive charge and some initial modeling results. Accepted: 9th International Symposium on Rock Fragmentation by Blasting, Madrid.

Krasnov, Y.K. (1981) Action of propellants and high explosives on rock. Soviet Mining Science. 17(1): 39-44.

Kuznetsov, V.M. (1974) Hydrodynamic calculation for ejection blasting by long charges. Soviet Mining Science. 10(3): 292-295.

Kuznetsov, V.M. (1977) Mathematical Models of Explosions. Nauka, Novosibirsk,

Mark C. & A. Iannacchione (2001) Ground Control Issues for Professionals. In: Mine Health and Safety Management (Ed.: Karmis, K.), p. 347-367, The Society for Mining Metallurgy and Exploration Inc., Colorado.

Mine Safety and Health Administration (MSHA) (1986-2006). Summary of selected Accidents/Injuries/Illnesses and Employment Data reported to MSHA under 30 CFR Part 50, Mine Injury and Worktime Quarterly and Self Extracting Files, 1986-2006. [www.msha.gov/ACCINJ/accinj.htm] and [www.msha.gov/STATS/PART50/p50y2k/p50y2k.HTM]. U.S. Department of Labor, Mine Safety and Health Administration, Office of Injury and Employment Information, Denver CO.

Nieman, I.B. (1976) Determination of the dimensions of the crushing in bounded rock massif due to the explosion of a cylindrical loosening charge. PhD. Thesis, Novosibirsk.

Nieman, I.B. (1979) Determination of the zone of crushing of rock in place by blasting. Soviet Mining Science, 15(5): 480-485.

Nieman, I.B. (1984a) Mathematical model of the explosive action of a fracturing charge in a ledge rock mass. Soviet Mining Science, 19(6): 494-499.

Nieman, I.B. (1984b) Correction of the hole charge parameters in rock bench breaking. Soviet Mining Science, 20(5): 385-388.

Nieman, I.B. (1986a) Modeling the explosion of a system of borehole charges in a scarp. Soviet Mining Science, 22(2): 108-113.

Nieman, I.B. (1986b) Volume models of the action of cylindrical-charge explosion in rock, Soviet Mining Science, 22(6): 455-463.

Vlasov, O.E. (1957) Principles of the theory of action of explosives. VIA, Moscow.

Vlasov, O.E. & S.A. Smirnov (1962) Fundamentals of Calculating the Crushing of Rocks Under the Actions of Explosives. Izd. Akad. Nauk SSSR, Moscow.

APPENDIX A - Limiting Damage Distance

If a relationship between the degree of damage and PPV has been established for the particular rock mass using some technique, it is of interest to be able to easily determine the corresponding extent of damage. To do this, one begins by writing Equation (16),

$$\rho = \frac{\sqrt{v_s}\,\bar{r}\sqrt{\bar{r}^2 + \frac{\bar{L}^2}{4}}}{\bar{L}}; \qquad (16)$$

in the form

$$\bar{r}^4 + \frac{\bar{L}^2}{4}\bar{r}^2 - \frac{\rho^2\,\bar{L}^2}{v_s} = 0. \qquad (A1)$$

Equation (A1) is a bi-quartic equation that can be solved by substituting $\bar{R}$ for $\bar{r}^2$. One obtains

$$\bar{R}^2 + \frac{\bar{L}^2}{4}\bar{R} - \frac{\rho^2\,\bar{L}^2}{v_s} = 0. \qquad (A2)$$

The two roots of Equation (A2) can be found by using the quadratic equation:

$$\bar{R}_1 = \frac{-\frac{\bar{L}^2}{4} + \sqrt{\frac{\bar{L}^4}{16} + \frac{4\rho^2\bar{L}^2}{v_s}}}{2} \quad \text{(A3)}$$

and

$$\bar{R}_2 = \frac{-\frac{\bar{L}^2}{4} - \sqrt{\frac{\bar{L}^4}{16} + \frac{4\rho^2\bar{L}^2}{v_s}}}{2}, \quad \text{(A4)}$$

where

$\bar{R}_1$, $\bar{R}_2$ are the roots of Equations (A3) and (A4).

The four roots of Equation (A1) are:

$$\bar{r}_1 = \sqrt{\bar{R}_1}, \quad \text{(A5)}$$

$$\bar{r}_2 = -\sqrt{\bar{R}_1}, \quad \text{(A6)}$$

$$\bar{r}_3 = \sqrt{\bar{R}_2}, \text{ and} \quad \text{(A7)}$$

$$\bar{r}_4 = -\sqrt{\bar{R}_2}. \quad \text{(A8)}$$

Equation (A5) is used for this application because Equation (A6) produces a negative number and Equations (A7) and (A8) produce imaginary numbers. The appropriate equation is

$$\bar{r}_1 = \left(\frac{-\frac{\bar{L}^2}{4} + \sqrt{\frac{\bar{L}^4}{16} + \frac{4\rho^2\bar{L}^2}{v_s}}}{2} \right)^{0.5}. \quad \text{(A9)}$$

In practice, one determines the ρ_{lim} corresponding to the particular PPV value, PPV_{lim} by using the crushing or cracking limit in Equation (17) and taking the inverse, which gives

$$\rho_{lim} = \left(\frac{PPV_{lim}}{I_f} \right)^{\frac{-1}{\alpha}}, \quad \text{(A10)}$$

where PPV_{lim} is the crushing or cracking limit.

One then substitutes ρ_{lim} for ρ in Equation (A9) to determine $\bar{r}_{1\,lim}$. The extent of damage r_{lim} corresponding to PPV_{lim} is then

$$r_{lim} = d \cdot \bar{r}_{1\,lim}. \tag{A11}$$

To demonstrate the use of this technique using the properties and explosive for the concrete block test, the limiting PPV for crushing, 4.45 m/s, is substituted into Equation (A10):

$$\rho_{lim} = \left(\frac{4.45}{414}\right)^{\frac{-1}{1.416}} = 24.56. \tag{A12}$$

For
L = 1.2 m,
d = 0.038 m, and
v_s = 8.29,

Equation (A9) becomes

$$\bar{r}_{1\,lim} = \left(\frac{\frac{-31.58^2}{4} + \sqrt{\frac{31.58^4}{16} + \frac{4\ x\ 24.56^2\ x\ 31.58^2}{8.29}}}{2} \right)^{0.5} = 13.1 \tag{A13}$$

Multiplying $\bar{r}_{1\,lim}$ by the charge diameter,

$$r_{lim} = 0.038m \cdot 13.1 = 0.5m \tag{A14}$$

which is the limiting distance corresponding to the limiting crushing velocity.

Applying the same technique for d = 76 mm yields 0.83 m for r_{lim}. The calibration method yielded 0.82 m for r_{lim} for this case.